

Microscopic membrane elasticity and interactions among membrane inclusions: interplay between the shape, dilation, tilt and tilt-difference modes

Jean-Baptiste FOURNIER

Laboratoire de Physico-Chimie Théorique, E. S. P. C. I. , 10 rue Vauquelin, 75231 Paris Cédex 05, France.

Received: date / Revised version: date

Abstract. A phenomenological Landau elasticity for the shape, dilation, and lipid-tilt of bilayer membranes is developed. The shape mode couples with the sum of the monolayers' tilt, while the dilation mode couples with the difference of the monolayers' tilts. Interactions among membrane inclusions within regular arrays are discussed. Inclusions modifying the membrane thickness and/or inducing a tilt-difference due to their convex or concave shape yield a dilation-induced attraction and a tilt-difference-induced repulsion. The resulting interaction can stabilize $2D$ crystal phases, with the possible coexistence of different lattice spacings when the dilation-tilt-difference coupling is large. Inclusions favoring crystals are those with either a long-convex or a short-concave hydrophobic core. Inclusions inducing a local membrane curvature due to their conical shape repel one another. At short inclusions separations, a tilt comparable with the inclusion's cone angle develops: it relaxes the membrane curvature and reduces the repulsion. At large separations the tilt vanishes, whatever the value of the shape-tilt coupling.

PACS. 34.20-b – 82.65Dp – 87.22Bt

1 Introduction

Bilayer membranes are formed by the self-assembly of amphiphilic molecules in water of brine [1]. The aliphatic chains of the constituent molecules condense into an oily sheet that is shielded from contact with water by the polar heads of the molecules. Membranes can form various phases, e.g., lamellar (L_α), vesicular (L_4), or sponge (L_3) phases [2,3]. Being self-assembled systems with a conserved area, it is essentially the competition between their curvature energy and their entropy that determines their large scale behavior. In the standard macroscopic theory, membranes are modeled as structureless surfaces with a curvature elasticity [4,5]. This description, which has the advantage to involve only two material constants, accounts for a large number of universal properties and behaviors of amphiphilic membranes [2,3,6].

On the other hand, a number of attempts have been made toward a more *microscopic* description of membranes [7,8,9,10,11,12]. The goal being to take into account various structural parameters of the bilayer, such as its thickness, the ordering of the chain segments, etc. As far as large scale properties are concerned, these extra degrees of freedom are irrelevant since they relax over microscopic lengths. Nevertheless, they can dictate important physical properties, such as adhesion behaviors, the short-range interaction between membrane inclusions, their aggregation

properties, phase behaviors, etc. The aim of this work is to construct an elastic model of membranes that connects microscopic and macroscopic descriptions. Beside the standard shape and dilation variables we shall consider as elastic variables the *tilts* of the lipids in both monolayers [13, 14]. The model will be used to investigate the role of the monolayers tilts in the interaction between membrane inclusions.

2 Elastic model

To construct an elastic model, one considers a distortion free energy depending on a particular set of structural parameters. Implicitly, this free energy results from the integration over all the microscopic states compatible with these (fixed) parameters of the Boltzmann weight associated with the microscopic Hamiltonian of the system. In practice, based on the symmetries of the system, one writes an expansion in powers of the structural parameters and their gradients. The choice of the relevant parameters depends on which deformations can be imposed externally on the system. We shall consider four structural parameters: (1) the membrane thickness, which can be modified, e.g., by the presence of an integral protein, (2) the membrane average shape, in order to connect with the large-scale theory and because it can be excited by a conically shaped inclusion, and (3) the tilts of the molecules within

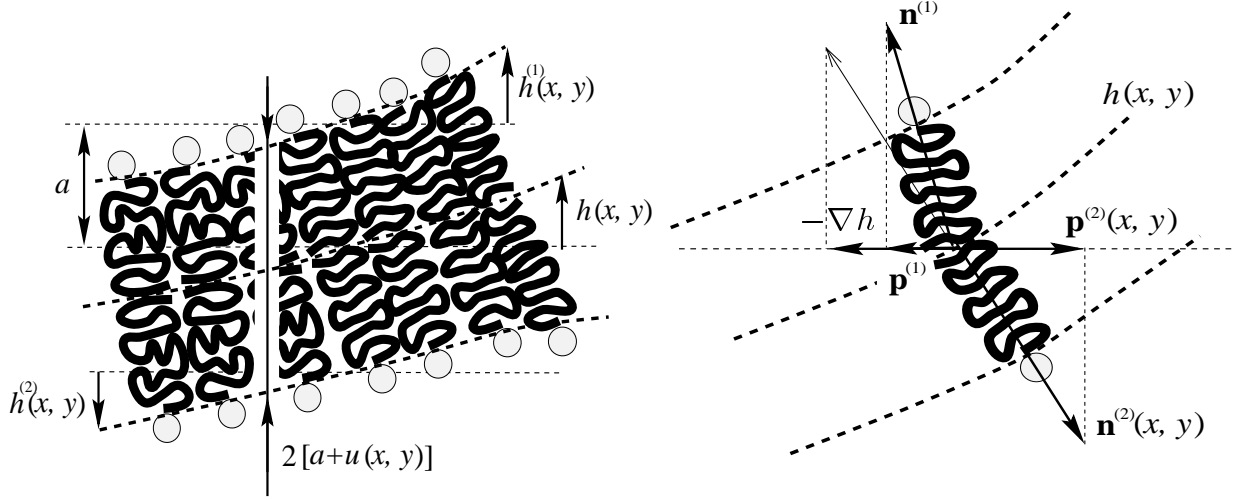


Fig. 1. a) Average membrane shape, h , and dilation, u , variables. b) Construction of the membrane average tilt $\mathbf{m} = \frac{1}{2}(\mathbf{p}^{(1)} + \mathbf{p}^{(2)}) + \nabla h$ and tilt-difference $\hat{\mathbf{m}} = \frac{1}{2}(\mathbf{p}^{(1)} - \mathbf{p}^{(2)})$ variables.

each monolayer, that can be independently excited by an inclusion with, e.g., a diamond-like shape.

To simplify, we assume that the membrane undergoes only small deviations with respect to its flat ground state. We denote by $h^{(1)}(x, y)$ and $h^{(2)}(x, y)$ the vertical displacements (along z) of the chain-water interfaces of the upper and lower monolayer, respectively, with respect their positions in the flat unperturbed state (Fig. 1a). For further use, let us define the average *shape* $h(x, y)$ and the membrane *dilation* by

$$h = \frac{h^{(1)} + h^{(2)}}{2} \quad (1)$$

$$u = \frac{h^{(1)} - h^{(2)}}{2}. \quad (2)$$

To construct the tilt variables, we introduce the vectors $\mathbf{p}^{(1)}(x, y)$ and $\mathbf{p}^{(2)}(x, y)$ defined in both monolayers as the projections onto the (x, y) plane of the unit vectors parallel to the molecular direction and oriented from chain to polar head (Fig. 1b). The tilts relative to the membrane normal are measured by $\mathbf{m}^{(1)} = \mathbf{p}^{(1)} + \nabla h$ and $\mathbf{m}^{(2)} = \mathbf{p}^{(2)} - \nabla h$. Let us define the *average tilt* $\mathbf{m}(x, y)$ and the *tilt-difference* $\hat{\mathbf{m}}(x, y)$ by

$$\mathbf{m} = \frac{\mathbf{m}^{(1)} + \mathbf{m}^{(2)}}{2}, \quad (3)$$

$$\hat{\mathbf{m}} = \frac{\mathbf{m}^{(1)} - \mathbf{m}^{(2)}}{2}. \quad (4)$$

2.1 Shape and dilation distortion energy

We start by constructing the most general quadratic free energy expansion in powers of $h^{(1)}$ and $h^{(2)}$ and its first and second gradient,

$$h^{(\alpha)}; \quad h_{,i}^{(\alpha)}; \quad h_{,ij}^{(\alpha)}. \quad (5)$$

Here, $\alpha = 1, 2$ is the monolayer label, and the comma denotes partial derivation with respect to the coordinates x and y . We write the free energy as $F = F^{(1)} + F^{(2)} + F^{(12)}$ with all the interaction terms coupling $h^{(1)}$ and $h^{(2)}$ in $F^{(12)}$. The symmetry of the bilayer imposes invariance with respect to the transformation:

$$h^{(1)} \rightarrow -h^{(2)}, \quad h^{(2)} \rightarrow -h^{(1)}. \quad (6)$$

Therefore, the most general quadratic form for $F^{(\alpha)}$ is

$$\begin{aligned} F^{(\alpha)} = & (-1)^\alpha a_1 h^{(\alpha)} + (-1)^\alpha a_2 h_{,ii}^{(\alpha)} + a_3 h^{(\alpha)2} \\ & + a_4 h^{(\alpha)} h_{,ii}^{(\alpha)} + a_5 h_{,i}^{(\alpha)} h_{,i}^{(\alpha)} + a_6 h_{,ii}^{(\alpha)2} \\ & + a_7 h_{,ij}^{(\alpha)} h_{,ij}^{(\alpha)}, \end{aligned} \quad (7)$$

summation over repeated indices being understood. The interaction energy, containing all the bilinear scalars, has the form

$$\begin{aligned} F^{(12)} = & b_1 h^{(1)} h^{(2)} + b_2 \left(h^{(1)} h_{,ii}^{(2)} + h^{(2)} h_{,ii}^{(1)} \right) \\ & + b_3 h_{,i}^{(1)} h_{,i}^{(2)} + b_4 h_{,ii}^{(1)} h_{,jj}^{(2)} + b_5 h_{,ij}^{(1)} h_{,ij}^{(2)}. \end{aligned} \quad (8)$$

Expressing now F in terms of h and u , we obtain the decoupled form $F = F_h + F_u$, with

$$\begin{aligned} F_h = & d_1 h^2 + d_2 h_{,i} h_{,i} + d_3 h h_{,ii} + d_4 h_{,ii}^2 \\ & + d_5 h_{,ij} h_{,ij} \end{aligned} \quad (9)$$

$$\begin{aligned} F_u = & e_1 u + e_2 u^2 + e_3 u_{,i} u_{,i} + e_4 u_{,ii} + e_5 u u_{,ii} \\ & + e_6 u_{,ii}^2 + e_7 u_{,ij} u_{,ij}. \end{aligned} \quad (10)$$

The new coefficients are related to the former by an invertible linear transformation. In this expression, several terms obviously vanish and other can be discarded: $e_1 \equiv 0$, since the minimum energy corresponds to $u = 0$ by construction; $d_1 = d_3 \equiv 0$ since F must be invariant under a translation. We shall set $d_2 = 0$, since the tension of membranes usually vanishes [15, 3]. There is no reason however

to discard the term $e_3(\nabla u)^2$, which represents the energy density associated with a *gradient of the membrane thickness*. The latter term involves not only the extra coast of lengthening the chain–water interfaces but also that of modulating the stretching of the molecules chains. Considers a planar membrane with a thickness modulation at some wavevector q : its elastic energy may be well described by the term $\propto u^2$ as long as $qa \ll 1$ (a monolayer thickness), however the term $\propto (\nabla u)^2$ should not be neglected when $qa \approx 1$. From this point of view the present model differs from those of Refs. [9, 10, 11, 12] that neglect the coefficient e_3 [16].

We can now rewrite F in a more traditional way. Relabeling the nonzero coefficients, and making use of $h_{,ij} h_{,ij} = (\nabla^2 h)^2 - 2 \text{Det}(h_{,ij})$, we arrive at

$$F_h = \frac{1}{2} \kappa (\nabla^2 h)^2 + \bar{\kappa} \text{Det}(h_{,ij}), \quad (11)$$

$$F_u = \frac{1}{2} B u^2 + \frac{1}{2} \lambda (\nabla u)^2 + \sigma \nabla^2 u + \sigma' u \nabla^2 u + \frac{1}{2} \kappa' (\nabla^2 u)^2 + \bar{\kappa}' \text{Det}(u_{,ij}). \quad (12)$$

F_h is simply the Helfrich energy [4, 5], in which $\nabla^2 h$ is twice the mean curvature of the average membrane shape, and $\text{Det}(h_{,ij})$ is its Gaussian curvature. The thickness variations, which are completely decoupled from the average membrane shape, are described by an energy F_u similar to that of Refs. [10, 11, 12], however with two important differences: (1) there is a non vanishing term $\propto (\nabla u)^2$ at lowest-order, (2) the bending constants κ' and $\bar{\kappa}'$ are different from the Helfrich constants appearing in F_h .

To further simplify our model, we shall discard the terms proportional to σ and σ' , since they can be transformed to boundary terms by integration by parts; we shall also discard the terms proportional to κ' and $\bar{\kappa}'$, in order to keep only the leading-order saturation terms. We are left (at the moment) with

$$F = \frac{1}{2} \kappa (\nabla^2 h)^2 + \bar{\kappa} \text{Det}(h_{,ij}) + \frac{1}{2} B u^2 + \frac{1}{2} \lambda (\nabla u)^2 \quad (13)$$

2.2 Tilt distortion energy and coupling terms

We expand the distortion energy associated with the tilts of the molecular orientation in powers of

$$m_i^{(\alpha)}; \quad m_{i,j}^{(\alpha)}; \quad (14)$$

The tilt gradient $m_{i,j}^{(\alpha)}$ is a non-symmetric second rank tensor. We write the tilt free energy as $G = G^{(1)} + G^{(2)} + G^{(12)} + G_{\text{int}}$ where all the terms coupling $\mathbf{m}^{(1)}$ and $\mathbf{m}^{(2)}$ are in $G^{(12)}$ and all the interaction terms coupling the tilts and the membrane shape or dilation are in G_{int} . The interaction can be divided into four contributions: $G_{\text{int}} = G_u^{(1)} + G_u^{(2)} + G_h^{(1)} + G_h^{(2)}$, each term containing all the contributions bilinear in either $m^{(1)}$ or $m^{(2)}$ and u or h . Because of the symmetry of the bilayer, we require invariance with respect to the transformation (6)

and the exchange of $\mathbf{m}^{(1)}$ and $\mathbf{m}^{(2)}$. Writing all the linear and quadratic scalars yields

$$G^{(\alpha)} = A_1 m_{i,i}^{(\alpha)} + A_2 m_i^{(\alpha)} m_i^{(\alpha)} + A_3 m_{i,i}^{(\alpha)2} + A_4 m_{i,j}^{(\alpha)} m_{i,j}^{(\alpha)} + A_5 m_{i,j}^{(\alpha)} m_{j,i}^{(\alpha)} \quad (15)$$

$$G^{(12)} = B_1 m_i^{(1)} m_i^{(2)} + B_2 m_{i,i}^{(1)} m_{j,j}^{(2)} + B_3 m_{i,j}^{(1)} m_{i,j}^{(2)} + B_4 m_{i,j}^{(1)} m_{j,i}^{(2)} \quad (16)$$

$$G_u^{(\alpha)} = C_1 m_i^{(\alpha)} u_{,i} + C_2 m_{i,i}^{(\alpha)} u + C_3 m_{i,i}^{(\alpha)} u_{,jj} + C_4 m_{i,j}^{(\alpha)} u_{,ij} \quad (17)$$

$$G_h^{(\alpha)} = (-1)^\alpha D_1 m_i^{(\alpha)} h_{,i} + (-1)^\alpha D_2 m_{i,i}^{(\alpha)} h + (-1)^\alpha D_3 m_{i,i}^{(\alpha)} h_{,jj} + (-1)^\alpha D_4 m_{i,j}^{(\alpha)} h_{,ij} \quad (18)$$

As previously, several terms can be discarded: $A_1 = C_2 = D_2 \equiv 0$, since we assume no spontaneous splay of the tilt; $D_1 \equiv 0$ since the minimum energy is still achieved with zero tilts when the membrane is rotated. We can also discard the terms with coefficients A_5 and B_4 : integrating them by parts merely yields boundary terms (and a renormalization of A_3 and B_2).

In terms of the variables \mathbf{m} and $\hat{\mathbf{m}}$, we can write the total tilt energy as $G = G_{\mathbf{m}} + G_{\mathbf{m}h} + G_{\hat{\mathbf{m}}} + G_{\hat{\mathbf{m}}u}$, with

$$G_{\mathbf{m}} = \frac{1}{2} t m_i m_i + k_1 m_{i,i}^2 + k_2 m_{i,j} m_{i,j} \quad (19)$$

$$G_{\mathbf{m}h} = d_3 m_{i,i} h_{,jj} + d_4 m_{i,j} h_{,ij} \quad (20)$$

$$G_{\hat{\mathbf{m}}} = \frac{1}{2} t' \hat{m}_i \hat{m}_i + k'_1 \hat{m}_{i,i}^2 + k'_2 \hat{m}_{i,j} \hat{m}_{i,j} \quad (21)$$

$$G_{\hat{\mathbf{m}}u} = c \hat{m}_i u_{,i} + c_1 \hat{m}_{i,i} u_{,jj} + c_2 \hat{m}_{i,j} u_{,ij}. \quad (22)$$

We can finally discard the terms with coefficients c_2 and d_4 by integrating by parts, and neglect the term with coefficient c_1 as a higher-order coupling term.

2.3 Total distortion energy

In vectorial notations and after some simple manipulations, the total distortion energy, i.e., $F + G$, can be written as $H_{hm} + H_{um}$, with

$$H_{hm} = \frac{1}{2} \kappa (\nabla^2 h)^2 + \bar{\kappa} \text{Det}(h_{,ij}) - \gamma \nabla^2 h (\nabla \cdot \mathbf{m}) + \frac{1}{2} t \mathbf{m}^2 + \frac{1}{2} K_1 (\nabla \cdot \mathbf{m})^2 + \frac{1}{2} K_2 (\nabla \times \mathbf{m})^2 \quad (23)$$

and

$$H_{um} = \frac{1}{2} B u^2 + \frac{1}{2} \lambda (\nabla u)^2 + c \nabla u \cdot \hat{\mathbf{m}} + \frac{1}{2} t' \hat{\mathbf{m}}^2 + \frac{1}{2} K'_1 (\nabla \cdot \hat{\mathbf{m}})^2 + \frac{1}{2} K'_2 (\nabla \times \hat{\mathbf{m}})^2 \quad (24)$$

The total energy therefore splits up into a contribution H_{hm} involving the average shape h and the average tilt \mathbf{m} , and a decoupled contribution H_{um} involving the dilation u and the tilt-difference $\hat{\mathbf{m}}$. The term with coefficient $\gamma > 0$

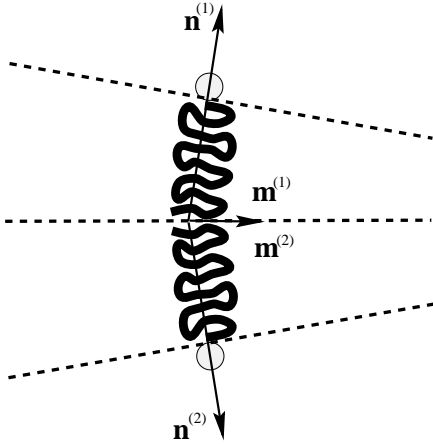


Fig. 2. Coupling between the tilt-difference $\hat{\mathbf{m}} = \frac{1}{2}(\mathbf{m}_1 + \mathbf{m}_2)$ and the thickness gradient ∇u , via the term $c \nabla u \cdot \hat{\mathbf{m}}$.

is responsible for the ripple phase of tilted membranes [17, 18]. Similarly, the term with coefficient c can produce a “ripple” instability in which a thickness modulation occurs together with a tilt-difference modulation [14]. From the tendency of the molecules to orient perpendicular to the chain–water interface we expect $c > 0$ (Fig. 2).

2.4 Equilibrium equations and energies

The total elastic energy of the membrane is given by

$$\mathcal{H} = \mathcal{H}_{hm} + \mathcal{H}_{u\hat{\mathbf{m}}} = \int d^2r H_{hm} + \int d^2r H_{u\hat{\mathbf{m}}}. \quad (25)$$

The equilibrium membrane configuration are those minimizing \mathcal{H} with respect to all possible local variations of the structural fields. The four corresponding Euler-Lagrange equations, namely $\delta\mathcal{H}/\delta h = 0$, $\delta\mathcal{H}/\delta \mathbf{m} = 0$, $\delta\mathcal{H}/\delta u = 0$ and $\delta\mathcal{H}/\delta \hat{\mathbf{m}} = 0$, are explicitly

$$\kappa \nabla^4 h = \gamma \nabla^2 (\nabla \cdot \mathbf{m}) \quad (26)$$

$$t \mathbf{m} - K_1 \nabla (\nabla \cdot \mathbf{m}) + K_2 \nabla \times (\nabla \times \mathbf{m}) = -\gamma \nabla (\nabla^2 h) \quad (27)$$

and

$$B u - \lambda \nabla^2 u = c \nabla \cdot \hat{\mathbf{m}} \quad (28)$$

$$t' \hat{\mathbf{m}} - K'_1 \nabla (\nabla \cdot \hat{\mathbf{m}}) + K'_2 \nabla \times (\nabla \times \hat{\mathbf{m}}) = -c \nabla u. \quad (29)$$

The calculation of the energy of equilibrium configurations can be simplified in the following way. Integrating $\mathcal{H}_{u\hat{\mathbf{m}}}$ by parts yields

$$\mathcal{H}_{u\hat{\mathbf{m}}} = \frac{1}{2} \int d^2r \left(u \frac{\delta \mathcal{H}}{\delta u} + \hat{\mathbf{m}} \cdot \frac{\delta \mathcal{H}}{\delta \hat{\mathbf{m}}} \right) + \mathcal{H}'_{u\hat{\mathbf{m}}} \quad (30)$$

with

$$\begin{aligned} \mathcal{H}'_{u\hat{\mathbf{m}}} = \frac{1}{2} \oint d\ell \mathbf{n} \cdot [& \lambda u \nabla u + c u \hat{\mathbf{m}} + K'_1 (\nabla \cdot \hat{\mathbf{m}}) \hat{\mathbf{m}} \\ & - K'_2 (\nabla \times \hat{\mathbf{m}}) \times \hat{\mathbf{m}}], \end{aligned} \quad (31)$$

where the last integral is restricted to the boundary of the integration domain, whose normal is \mathbf{n} . For equilibrium configurations, $\mathcal{H}_{u\hat{\mathbf{m}}}$ reduces to $\mathcal{H}'_{u\hat{\mathbf{m}}}$ since the first term of (30) vanishes. This provides a very useful simplification.

One finds similarly that \mathcal{H}_{hm} reduces for equilibrium configurations to

$$\begin{aligned} \mathcal{H}'_{hm} = \frac{1}{2} \oint d\ell \mathbf{n} \cdot [& \kappa \nabla^2 h \nabla h - \kappa h \nabla (\nabla^2 h) \\ & - \gamma (\nabla \cdot \mathbf{m}) \nabla h + \gamma h \nabla (\nabla \cdot \mathbf{m}) - \gamma (\nabla^2 h) \mathbf{m} \\ & + K_1 (\nabla \cdot \mathbf{m}) \mathbf{m} - K_2 (\nabla \times \mathbf{m}) \times \mathbf{m}] \end{aligned} \quad (32)$$

2.5 Orders of magnitude

For biological membranes, the bending constants $\kappa > 0$ and $\bar{\kappa} < 0$ have relatively high values $\simeq 10^{-12}$ erg ($\simeq 25 k_B T$) [1]. The typical value of the membrane area-stretching coefficient $k \simeq 100$ erg/cm² [1] allows to determine the dilation modulus via $B = k/(2a)^2$, where $a \simeq 20 \times 10^{-8}$ cm is a typical monolayer thickness. This yields $B \simeq 6 \times 10^{14}$ erg/cm⁴. Therefore $B \simeq \kappa/a^4$: the membrane has a typical energy scale given by κ and a typical length scale given by a . In the absence of experimental measurements, the other constants have to be estimated by dimensional analysis. We expect λ to be $\approx \kappa/a^2$ (we recall that λ is independent of the membrane tension). We therefore estimate $\lambda \approx 25$ erg/cm². Next, we shall assume roughly that tilting the molecules by a large angle compares energetically with compressing the membrane by half a monolayer thickness. This yields $t \approx t' \approx \lambda$. Then, we expect the characteristic length defined by the $(K_i/t)^{1/2}$ to be of order a , which implies $K_i \approx \lambda a^2 \approx 10^{-12}$ erg. This value correctly compares with the bending constant. Finally, the K'_i 's are expected to be of the same order of magnitude as the K_i 's, and c is dimensionally expected to compare with λ .

2.6 Remarks on the validity of the truncation of the energy expansion

Strictly speaking, in all the microscopic theories of membranes [8, 9, 10, 11, 12], it is somewhat arbitrary to truncate the expansion at the lowest-order in the derivatives of the distortion field. Indeed, since the typical energy and length scales of the membrane are κ and a , respectively, the distance ξ on which dilation perturbations relax is expected to be $\approx a$. For small distortions $u \ll a$ there is no problem in neglecting quartic terms such as the one $\sim (\nabla u)^4$: this term is $(u/a)^2$ times smaller than the leading term $\sim (\nabla u)^2$.

However the term $\sim (\nabla^2 u)^2$, which we have discarded, might be of the same order of magnitude as the leading term $\sim (\nabla u)^2$ if indeed its coefficient is $\simeq \kappa$. The problem is that all the terms $\sim (\nabla^n u)^2$ may be also comparable if their coefficients are $\simeq \kappa a^{2n-4}$. However, at the microscopic scale corresponding to a , the membrane is not

actually a continuum and there is not much meaning in considering high order derivatives of the thickness. It may therefore be a good approximation to keep only the leading order term.

In any case, we expect that the lowest-order truncation of this continuum description will give a correct physical picture, at least qualitatively, of the competing trends associated with the various elastic variables. Note also that the truncation may be technically correct in the vicinity of a transition to a more ordered L_β or L'_β phase with a different equilibrium thickness, where B might be significantly reduced and, accordingly, ξ larger than a .

3 Interactions among membrane inclusions

Biological membranes contain a large number of inclusions such as integral proteins. Inclusions with a conical shape tend to curve the membrane since the lipids orient parallel to the inclusion's boundary in order to fill the volume. Because of the interference between the resulting membrane distortions, such inclusions are subject to long-range interactions [19,20,21]. Inclusions also experience "Casimir" forces, which are due to the modification of the membrane fluctuation spectrum caused by their presence.

The *short-range* interactions between inclusions arise from the local structural changes that the latter impose on the membrane [7,8,9,10,11,12]. For instance, since proteins have a central hydrophobic region that spans the hydrophobic core of the membrane, a thickness mismatch between the hydrophobic region of the protein and that of the bilayer will result in a local membrane thickness perturbation. Interferences between such perturbations yield membrane-mediated interactions that add up to the standard screened-electrostatic and van der Waals interactions.

3.1 Boundary conditions

Let us consider a membrane inclusion such as the one depicted in Fig. 3. It is meant to model an integral protein with an arbitrary shape. For the sake of simplicity, however, we assume revolution symmetry. We suppose that the hydrophobic region of the inclusion has a thickness $2H$ that differs from the corresponding thickness $2a$ in the bilayer. The inclusion is also assumed to have a piecewise conical shape with two angles θ_1 and θ_2 pertaining to each monolayer and relative to the revolution axis.

Let us consider an undistorted reference membrane above which the inclusion stands at a height h_0 . As previously we denote by $h^{(1)}$ and $h^{(2)}$ the positions of the upper and lower membrane interfaces with respect to their equilibrium positions in the reference membrane. Assuming a strong coupling between hydrophobic parts [8,9,10,11,12], we require the conditions that both monolayers interfaces reach the inclusion at the separation line between its hydrophobic and hydrophilic regions, i.e.,

$$h^{(1)}|_{r_0} \simeq h_0 + H - a, \quad (33)$$

$$h^{(2)}|_{r_0} \simeq h_0 - (H - a). \quad (34)$$

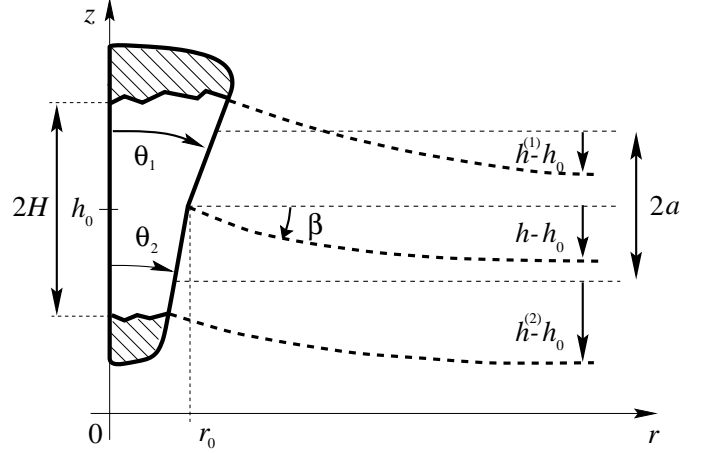


Fig. 3. General boundary conditions imposed by an inclusion.

These conditions are only approximate because the position where the interfaces reach the inclusion is equal to r_0 only at lowest order in the deformation variables. Another boundary "condition", which is not imposed but actually free to adjust to equilibrium, is the angle β at which the mid-membrane shape h departs from the inclusion. Calling \mathbf{e}_r the unit vector along r , this condition is

$$\nabla h|_{r_0} \simeq \beta \mathbf{e}_r. \quad (35)$$

If we now require that the molecules within the membrane lie parallel to the inclusion's boundary, because of the space-filling constraint, we have the condition

$$\mathbf{p}^{(1)}|_{r_0} \simeq -\theta_1 \mathbf{e}_r, \quad (36)$$

$$\mathbf{p}^{(2)}|_{r_0} \simeq \theta_2 \mathbf{e}_r. \quad (37)$$

Note that we have implicitly assumed that the revolution axis of the inclusion is normal to the reference plane (x, y) , although in the most general situation it can be a tilted (this tilt will be zero by symmetry in the following).

3.1.1 Decoupled boundary conditions

In order to make use of the equilibrium equations previously derived, we must transform these boundary conditions into conditions involving the variables h , u , \mathbf{m} , and $\hat{\mathbf{m}}$. From Eqs. (1-2) and Eqs. (3-4), we obtain

$$h|_{r_0} \simeq h_0, \quad (38)$$

$$\nabla h|_{r_0} \simeq \beta \mathbf{e}_r, \quad (39)$$

$$\mathbf{m}|_{r_0} \simeq (\beta - \Theta) \mathbf{e}_r, \quad (40)$$

and

$$u|_{r_0} \simeq u_0, \quad (41)$$

$$\hat{\mathbf{m}}|_{r_0} \simeq \alpha_0 \mathbf{e}_r, \quad (42)$$

where $\Theta = \frac{1}{2}(\theta_1 + \theta_2)$ is the average cone angle of the inclusion, $u_0 = H - a$ is the dilation and $\alpha_0 = \frac{1}{2}(\theta_2 - \theta_1)$ the tilt-difference set by the inclusion. It is important to note that these two sets of boundary conditions are decoupled in the same way as the corresponding equilibrium equations.

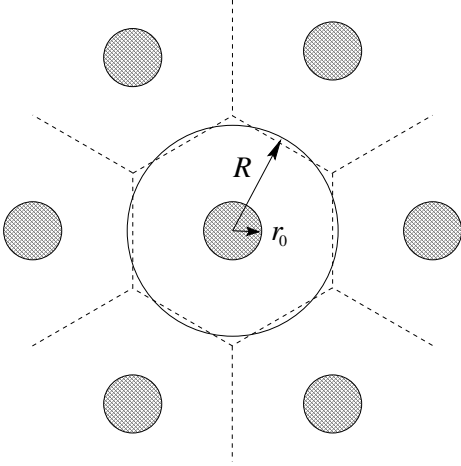


Fig. 4. An array of inclusions and its Wigner-Seitz cell.

3.1.2 Arrays of inclusions

Following previous works, we shall calculate the constitutive energy of *arrays* of inclusions. Paradoxically, it is easier to approximatively calculate the energy of an array than to calculate exactly the interaction between two inclusions. Since membrane-mediated interactions are not pairwise additive, this is the correct procedure to investigate the stability of 2D crystalline structures.

To capture the physics of an array of inclusions, the standard method is to consider a single inclusion surrounded by its Wigner-Seitz cell (i.e., the unit cell made by the perpendicular bisectors of the bonds connecting the lattice sites) [8,10,11,12]. The Wigner-Seitz cell is further idealized by a circle of radius approximatively half the inclusions separation (cf. Fig. 4), and the equilibrium equations are solved assuming *revolution symmetry*, with boundary conditions at $r = r_0$ and $r = R$. When applied to an hexagonal lattice of inclusions, this approximation is quite good, as it consists in neglecting high Fourier harmonics of order 6, 12, etc. In a gas of inclusions, it amounts to considering that the first neighbors effectively screen the other inclusions.

3.2 Dilation–tilt-difference induced interactions in an array of inclusions

Inclusions with arbitrary shapes will in general excite all of the four distortion modes considered in this work. However, since we have seen that both the equilibrium equations and the boundary conditions are pairwise decoupled, one can study separately, and simply add, the effects of the coupled dilation and tilt-difference modes and the effects of the coupled shape and tilt modes.

3.2.1 Zero dilation–tilt-difference coupling

We focus on the dilation (u) and tilt-difference ($\hat{\mathbf{m}}$) modes and, to start with, we neglect their coupling:

$$c = 0. \quad (43)$$

Let us consider an array of inclusions, and assume, as previously discussed, a perfect revolution symmetry in the Wigner-Seitz cell surrounding an inclusion:

$$u = u(r) \quad \text{and} \quad \hat{\mathbf{m}} = \alpha(r) \mathbf{e}_r. \quad (44)$$

Under these conditions, the most general solution of the equilibrium equations (28-29) takes the form

$$u(r) = \left[A_1 K_0\left(\frac{r}{\xi_u}\right) + A_2 I_0\left(\frac{r}{\xi_u}\right) \right] \times \sqrt{\frac{t'}{B}}, \quad (45)$$

$$\alpha(r) = \left[A_3 K_1\left(\frac{r}{\xi_\alpha}\right) + A_4 I_1\left(\frac{r}{\xi_\alpha}\right) \right], \quad (46)$$

in which the I's and the K's are modified Bessel function and

$$\xi_u = \sqrt{\frac{\lambda}{B}}, \quad (47)$$

$$\xi_\alpha = \sqrt{\frac{K'_1}{t'}}, \quad (48)$$

are two characteristic length comparable with the membrane thickness, except close to a L_β tilted phase where t' might be small, or close to the main-chain transition where B might be small. The constants A_i 's, which are real and dimensionless, are determined from the boundary conditions:

$$u|_{r_0} = u_0, \quad (49)$$

$$\alpha|_{r_0} = \alpha_0, \quad (50)$$

$$\dot{u}|_R = 0, \quad (51)$$

$$\alpha|_R = 0, \quad (52)$$

with a dot indicating derivation with respect to r . The quantities u_0 and α_0 are the boundary dilation and tilt-difference, respectively. The last two conditions are required by symmetry on the Wigner-Seitz circle.

Figure 5 shows a typical solution for an isolated inclusion ($R \rightarrow \infty$) and Fig. 6 shows a typical solution corresponding to an array of interacting inclusions. These pictures sketch the membrane structure: the solid line represents the membrane shape, i.e., the sum of the equilibrium monolayer thickness a and the thickness excess u . The dashed curve represents the amplitude of the tilt-difference angle α . For the sake of clarity the distortions have been amplified in the following way: the boundary angle α_0 , the equilibrium monolayer thickness a , and the boundary thickness excess u_0 are all normalized to 1.

Assuming revolution symmetry, the general distortion energy (31) within the Wigner-Seitz cell, takes the form

$$\mathcal{H}_{um} = \pi \left[\lambda r u \dot{u} + c r u \alpha + K'_1 r \alpha \dot{\alpha} + K'_1 \alpha^2 \right]_{r_0}^R, \quad (53)$$

in which several terms vanish due to the boundary conditions. After eliminating constant terms, \mathcal{H}_{um} reduces to

$$\mathcal{H}_{um} = \mathcal{H}_u + \mathcal{H}_m = -\pi r_0 (\lambda u_0 \dot{u}|_{r_0} + K'_1 \alpha_0 \dot{\alpha}|_{r_0}). \quad (54)$$

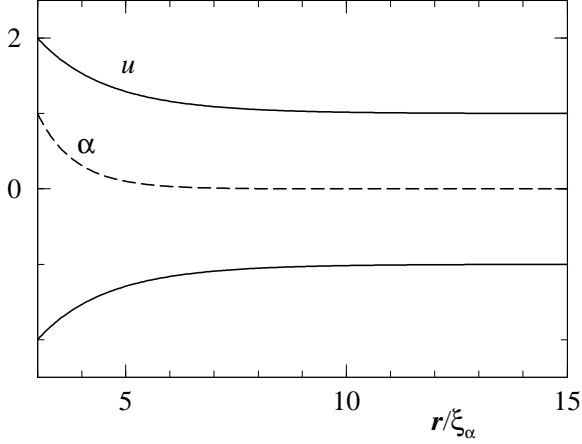


Fig. 5. Sketch of the membrane structure around an isolated inclusion (distortions are amplified, see text). The inclusion radius is $r_0 = 3\xi_\alpha (\simeq 60 \text{ \AA})$, $\xi_u/\xi_\alpha = 2$ and $c = 0$.

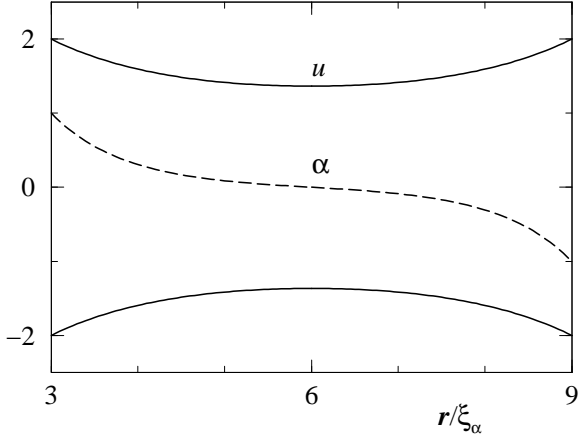


Fig. 6. Membrane structure between two inclusions in the array (amplified distortions). Parameters are as in Fig. 5.

This interaction, which in principle depends on a large number of parameters (r_0 , R , u_0 , α_0 , B , λ , t' and K') has the following scaling property:

$$\frac{\mathcal{H}_{um}}{\pi B r_0 \xi_\alpha u_0^2} = \overline{\mathcal{H}}_{um} \left(x^2, s, \frac{r_0}{\xi_\alpha}, \frac{R}{\xi_\alpha} \right), \quad (55)$$

$$s = \frac{\xi_u}{\xi_\alpha}, \quad (56)$$

$$x = \frac{\alpha_0}{u_0 \sqrt{B/t'}}, \quad (57)$$

which advantageously reduces the effective numbers of parameters. At short inclusions separations, \mathcal{H}_{um} diverges as $(R - r_0)^{-1}$ and \mathcal{H}_u goes to a negative constant. At large separations, both relax exponentially. Figure 7 shows a typical situation where an energy minimum appears, resulting from the superposition of a dilation-induced attraction, that dominates at large distances, and a tilt-difference-induced repulsion, that dominates at short distances. This situation manifests itself for large values of ξ_u , for which the dilation mode has the longest range, and for

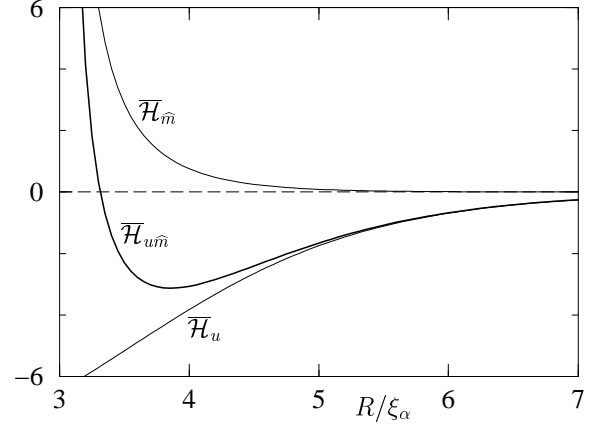


Fig. 7. Normalized interaction energy per inclusion $\overline{\mathcal{H}}_{um}$ vs. the inclusions separation R . The curves correspond to $r_0 = 3\xi_\alpha (\simeq 60 \text{ \AA})$, $s = 2$, $x = 1$ and $c = 0$. The normalized energies $\overline{\mathcal{H}}_u$ and $\overline{\mathcal{H}}_m$ correspond to the attractive dilation and repulsive tilt-difference contributions, respectively.

small values of the boundary tilt-difference α_0 , for which the repulsion is weak

Let us estimate the magnitude of the interaction energy, which is given by the normalization factor $\pi B r_0 \xi_\alpha u_0^2$ in (55). We choose for the tilt-difference coherence length a fixed microscopic value $\xi_\alpha \simeq 20 \text{ \AA}$ and we let for instance $0.1 < s < 10$. This assumption is based on the fact that close to the main chain transition ξ_u should exhibit some degree of pretransitional divergence. For the inclusion, we assume a typical protein size $r_0 = 3\xi_\alpha (\simeq 60 \text{ \AA})$ and a thickness perturbation $u_0 = 0.2\xi_\alpha (\simeq 4 \text{ \AA})$. With the estimated values of the material constants given in Sec. 2.5, we obtain $\pi B r_0 \xi_\alpha u_0^2 \simeq (10/s^2)k_B T$.

In the energy graphs depicted in Fig. 7, the values $x=1$ and $s=2$ correspond to an inclusion boundary tilt-difference angle $\alpha_0 = (x/s)(u_0/\xi_\alpha)\sqrt{\lambda/t'} \simeq 6^\circ$. The depth of the energy minimum is $3 \times \pi B r_0 \xi_\alpha u_0^2 \simeq 7 k_B T$. For such a well, we expect that the array of inclusion will crystallize, the distance between the boundaries of the particles being then $2(R - r_0) \simeq 2 \times 0.8\xi_\alpha \simeq 35 \text{ \AA}$ [22].

If we consider the inclusions radius r_0 as fixed, the interaction potential as a function of R depends only on the parameters x and s , as can be seen in (55). We have plotted in Fig. 8 the phase diagram, in the (x, s) plane, for a collection of identical inclusions. Distinction is made between a disordered (D) gaseous state and a crystal (K) phase. The criterion for the latter is the existence of a energy minimum with a depth larger than $k_B T$.

3.2.2 Nonzero dilation–tilt-difference coupling

In order to study the effect of the dilation–tilt-difference coupling, we now assume

$$c \neq 0, \quad \text{and} \quad \xi_u = \xi_\alpha \equiv \xi. \quad (58)$$

The latter condition is a simplification, which is reasonable far from any membrane phase transition (with ξ of

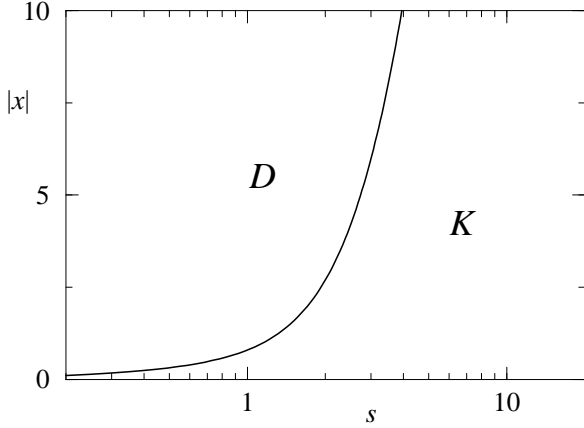


Fig. 8. Phase diagram for a membrane with $\xi_\alpha \simeq 20 \text{ \AA}$ containing dilation-tilt-difference inducing inclusions with radius $r_0 = 3 \xi_\alpha (\simeq 60 \text{ \AA})$. The coupling c is neglected. (D) disordered phase. (K) crystal phase, as determined from the existence of an energy minimum deeper than $k_B T$.

the order of the membrane thickness). Let us define the coupling's characteristic length as

$$\ell = \frac{c}{2\sqrt{Bt'}}. \quad (59)$$

We assume $\ell < \xi$, otherwise the membrane undergoes the microscopic “ripple” instability already mentioned [14].

Under the revolution symmetry conditions (44), the most general solution of the equilibrium equations (28-29) is given by the real part of

$$u(r) = \left[A_1 K_0 \left(e^{i\phi} \frac{r}{\xi} \right) + A_2 I_0 \left(e^{i\phi} \frac{r}{\xi} \right) \right] \times \sqrt{\frac{t'}{B}}, \quad (60)$$

$$\alpha(r) = \left[A_1 K_1 \left(e^{i\phi} \frac{r}{\xi} \right) - A_2 I_1 \left(e^{i\phi} \frac{r}{\xi} \right) \right] \times i, \quad (61)$$

where $i = \sqrt{-1}$, A_1 and A_2 are two dimensionless *complex* constants, and

$$\sin \phi = \frac{\ell}{\xi}. \quad (62)$$

The constants A_1 and A_2 are determined from the boundary conditions (49–52) as previously. Figures 9 and 10 show a typical solution for an isolated inclusion ($R \rightarrow \infty$) and a typical solution for interacting inclusions, respectively. The same conventions as for Figs. 5 and 6 are used.

The distortion energy within the Wigner-Seitz cell is given by exactly the same formula (54) as previously. Indeed, although the second term of (53) does not vanish any longer in $r = r_0$, it is constant and can be omitted in the interaction. Note however that this energy cannot be splitted any longer into pure dilation and tilt-difference contributions. Again, \mathcal{H}_{um} has the following scaling property:

$$\frac{\mathcal{H}_{um}}{\pi B r_0 \xi u_0^2} = \overline{\mathcal{H}}_{um} \left(x, \phi, \frac{r_0}{\xi}, \frac{R}{\xi} \right). \quad (63)$$

Depending on the values of r_0/ξ , x and ϕ , the interaction energy is either monotonically repulsive or exhibits one or

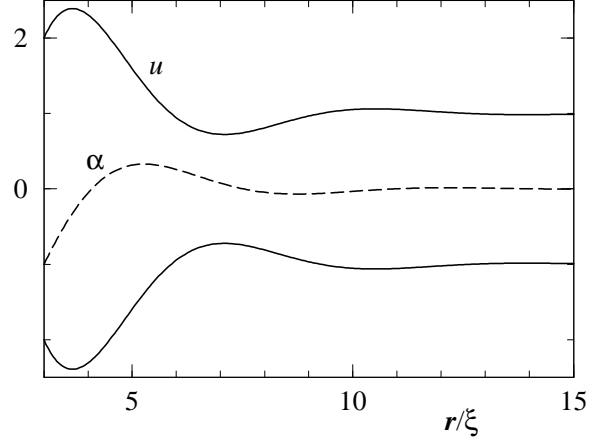


Fig. 9. Sketch of the membrane structure around an isolated inclusion (amplified distortions). The inclusion radius is $r_0 = 3 \xi (\simeq 60 \text{ \AA})$, $x = -2$, and $\phi = 0.75 \times \pi/2$.

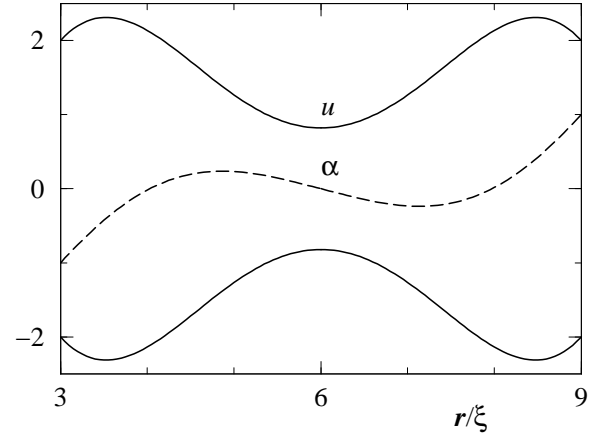


Fig. 10. Membrane structure between two inclusions in the lattice (amplified distortions). Parameters are as in Fig. 9.

several marked minima. Figure 11 shows a typical situation in which two minima appear. This phenomenon manifests itself for values of the dilation-tilt-difference coupling corresponding to $\phi > 0.6 \times \pi/2$, where, because of the vicinity of the dilation-tilt-difference “ripple” instability, the membrane has a tendency to develop damped undulations.

The magnitude of the interaction energy is now given by the normalization factor $\pi B r_0 \xi u_0^2$. With typically $\xi \simeq 20 \text{ \AA}$, and again $r_0 = 3 \xi (\simeq 60 \text{ \AA})$, $u_0 = 0.2 \xi (\simeq 4 \text{ \AA})$, we obtain, with the values of the material constants estimated in Sec. 2.5, the typical energy scale $\pi B r_0 \xi u_0^2 \simeq 10 k_B T$. The boundary tilt-difference angle is then given by $\alpha_0 = x u_0 \sqrt{B/t'} \simeq x u_0 / \xi \simeq x \times 10^\circ$ (for $\lambda \simeq t'$ as consistently assumed in Sec. 2.5). Therefore, in Fig. 11, the depths of the two minima are $\simeq 25 k_B T$ and $\simeq 3 k_B T$, respectively. Two distinct crystals might therefore appear: one with a distance between the boundaries of the particles of $2(R - r_0) \simeq 2 \times 1.2 \xi \simeq 50 \text{ \AA}$, the other with a much larger separation $2(R - r_0) \simeq 2 \times 4.5 \xi \simeq 180 \text{ \AA}$ [22].

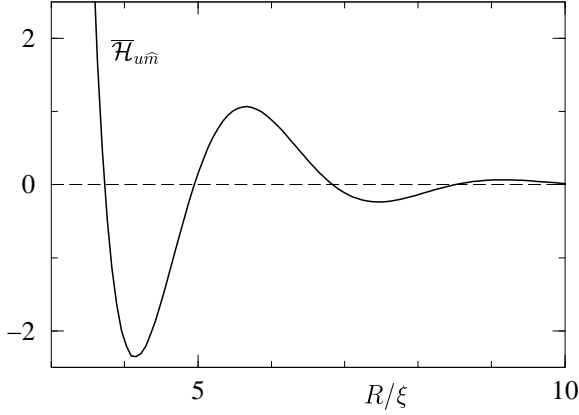


Fig. 11. Normalized interaction energy per inclusion $\hat{\mathcal{H}}_{um}$ vs. the inclusions separation R . The curves correspond to $r_0 = 3\xi$ ($\simeq 60$ Å), $x = -3$, and $\phi = 0.75 \times \pi/2$.

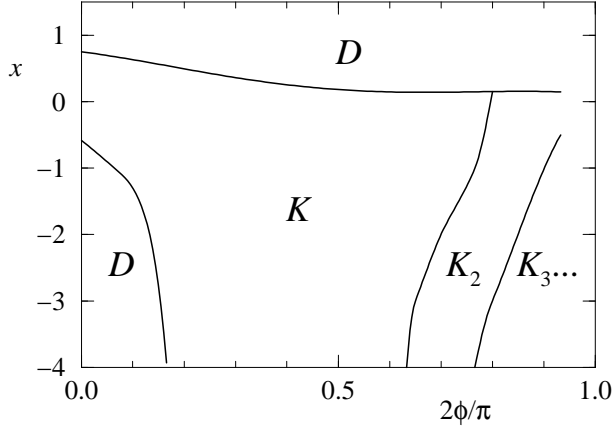


Fig. 12. Phase diagram for a membrane with $\xi \simeq 20$ Å containing dilation-tilt-difference inducing inclusions with radius $r_0 = 3\xi_\alpha$ ($\simeq 60$ Å). (D) disordered phase. (K) crystal phase, (K_n) region where n possible distinct crystalline phases with different particles separations are possible.

If we consider the inclusions radius r_0 as fixed, the interaction potential as a function of R depends only on the parameters x and ϕ , as can be seen from (63). Figure 12 shows a phase diagram in the (x, ϕ) plane for a collection of identical inclusions. The symbol (D) indicates a disordered (D) gaseous state, (K) a crystal phase, and (K_n) the possibility of n distinct crystalline phases with different separation distances. Again, the criterion for any crystal phase is an energy minimum depth larger than $k_B T$.

An interesting feature of the phase diagram of Fig. 12 is the asymmetry with respect to the change $x \leftrightarrow -x$ introduced by the dilation-tilt-difference coupling: crystal phases are more likely to occur for $x < 0$, i.e., for a *thick-convex* inclusion ($u_0 > 0$ and $\alpha_0 < 0$) or for a *thin-concave* inclusion ($u_0 < 0$ and $\alpha_0 > 0$). This symmetry-breaking follows from the sign $c > 0$ of the dilation-tilt-difference coupling, that we have assumed, in order to favor the situation depicted in Fig. 2.

This asymmetry can be explained by simple arguments. First, let us recall that if a non-zero boundary tilt-difference

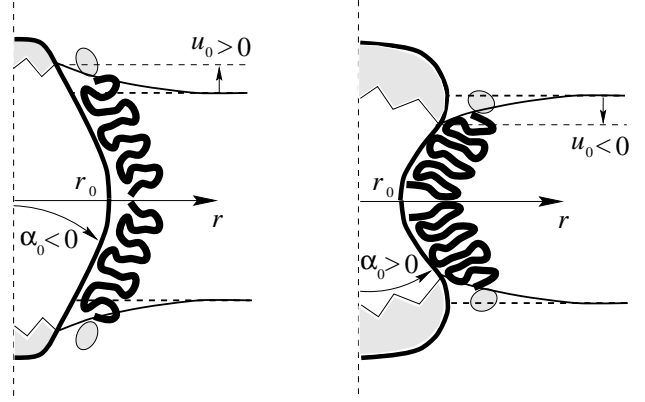


Fig. 13. Sketch of the inclusions that tend to form 2D crystals ($x < 0$). The dashed lines show the monolayers of the unperturbed membrane. (Left) Thick-convex inclusion ($u_0 > 0$ and $\alpha_0 < 0$). (Right) Thin-concave inclusion ($u_0 < 0$ and $\alpha_0 > 0$).

α_0 is present, the interaction is always repulsive at short distances. Indeed, the tilt-difference must go from α_0 to $-\alpha_0$ from one inclusion to the other. Conversely, the distortion associated with the membrane dilation is attractive since the thickness mismatch is the same on identical inclusions. Two situations are therefore possible: if the dilation relaxes on a longer range than the tilt-difference, a crystal phase can occur since there is a long-range attraction followed by a short-range repulsion, whereas conversely the repulsion simply dominates. We therefore have to understand how the coupling affects the relative range of the dilation and tilt-difference distortions. To simplify, let us rewrite schematically the interaction energy (24) as

$$\mathcal{H}_{um} \sim u^2 + \xi^2 \dot{u}^2 + \dot{u}\alpha + \alpha^2 + \xi^2 \dot{\alpha}^2, \quad (64)$$

Let us first assume $u_0, \alpha_0 > 0$, which corresponds to $x > 0$. To relax the positive dilation u_0 , the membrane will set $\dot{u} < 0$. The term $\dot{u}\alpha$ being then negative, it reduces the cost of making a gradient of u . Therefore the u distortion will relax on distance that is somewhat *shorter* than ξ : the attractive dilation tail retracts (see Fig. 14). From the point of view of the tilt-difference, since $\dot{u} < 0$, the coupling $\dot{u}\alpha$ makes it as if the potential was of the type $(\alpha - \alpha_m)^2$ with $\alpha_m > 0$. Thus, on the distance ξ , the tilt-difference relaxes only up to α_m ; it therefore needs a *longer* distance to reach zero: the repulsive tilt-difference tail expands (see Fig. 14). Then, for $x > 0$, a disordered phase is more favored, since the repulsive tail dominates at large distances.

With still $u_0 > 0$, let us now assume $\alpha_0 < 0$, corresponding to $x < 0$. Now the term $\dot{u}\alpha$ is positive: building a gradient of u is more costly and therefore the attractive dilation tail expands (see Fig. 15). The tilt-difference, however, still experiences a potential of the type $(\alpha - \alpha_m)^2$ with $\alpha_m > 0$, but it now starts from a negative value α_0 . On a distance ξ it would reach the equilibrium value $\alpha_m > 0$, it therefore reaches zero on a distance now shorter than ξ : the repulsive tilt-difference tail retracts (cf. Fig. 15). Thus, for $x < 0$, a crystal phase is more favored, since the attractive tail dominates at large distances (and then the repulsive one at short distances).

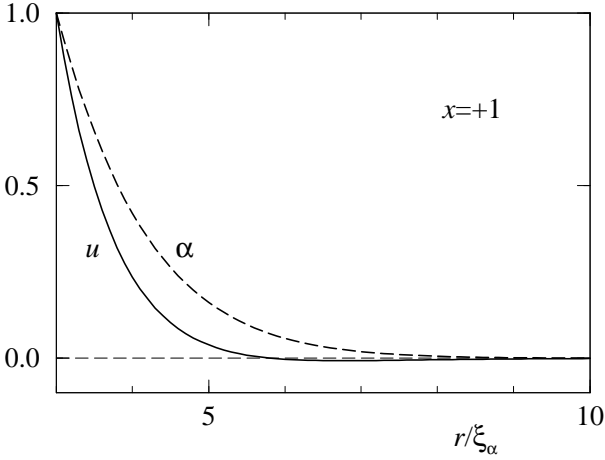


Fig. 14. Dilation and tilt-difference distortions around an isolated inclusion with $x > 0$. The inclusion radius is $r_0 = 3\xi (\simeq 60 \text{ \AA})$ and the coupling corresponds to $\phi = 0.2 \times \pi/2$. Due to the latter, the tilt-difference tail expands (dashed line) and the dilation tail retracts (solid line), thereby favoring repulsion, i.e., a disordered phase.

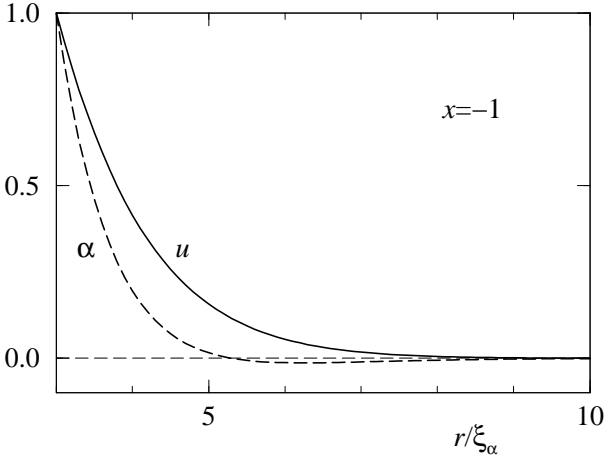


Fig. 15. Same as Fig. 14 but for $x < 0$. Now the tilt-difference tail retracts and the dilation tail expands, thereby favoring attraction, i.e., a crystal phase.

3.3 Shape-tilt induced interactions in an array of inclusions

We now focus on the shape (h) and tilt (\mathbf{m}) distortion modes induced by the inclusions. Assuming again revolution symmetry in the Wigner-Seitz cell,

$$h = h(r) \quad \text{and} \quad \mathbf{m} = \theta(r) \mathbf{e}_r, \quad (65)$$

the most general solution of the equilibrium equations (26-27) takes the form

$$h = (ar^2 + b) \log r + cr^2 + d + A I_0(qr) + B K_0(qr), \quad (66)$$

$$\theta = -4 \frac{L^2 a}{\mu r} + \frac{qA}{\mu} I_1(qr) - \frac{qB}{\mu} K_1(qr), \quad (67)$$

with

$$\mu = \frac{\gamma}{\kappa}, \quad (68)$$

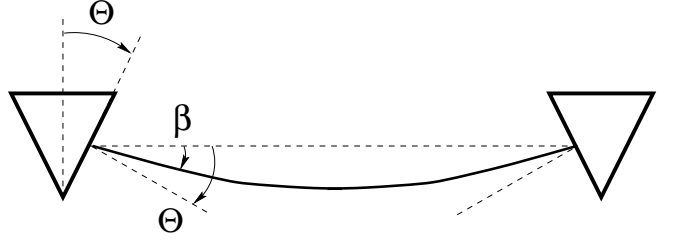


Fig. 16. Sketch of the membrane mid-surface shape (h) between conical inclusions. The tilt of the lipid molecules at the inclusion boundary is $\beta - \Theta$.

$$L = \frac{\gamma}{\sqrt{t\kappa}}, \quad (69)$$

$$\xi_\theta = \sqrt{\frac{K_1}{t}}, \quad (70)$$

$$q^{-1} = \sqrt{\xi_\theta^2 - L^2}. \quad (71)$$

We assume $L < \xi_\theta$, i.e., $\gamma^2 > K\kappa$, otherwise the membrane undergoes the ripple instability of the $P_{\beta'}$ phase, in which undulations and periodic tilt distortions occur [17, 18]. We assume also $L > 0$, i.e., $\gamma > 0$, since we expect the molecules to tilt in such a way as to *relax* the splay of the molecules in a curved membrane.

To simplify, let us assume strictly $K_1 = \kappa$. We then have $L = \mu \xi_\theta$. Hence $0 < \mu < 1$ is now the only parameter controlling the shape-tilt coupling. The six real unknowns a, b, c, d, A , and B are determined, according to the general boundary conditions (38-40) for an inclusion with average cone angle Θ , by

$$h|_{r_0} = h_0, \quad (72)$$

$$\dot{h}|_{r_0} = \beta, \quad (73)$$

$$\theta|_{r_0} = \beta - \Theta, \quad (74)$$

$$h|_R = h_0, \quad (75)$$

$$\dot{h}|_R = 0, \quad (76)$$

$$\theta|_R = 0. \quad (77)$$

The latter three conditions are required by symmetry on the Wigner-Seitz circle, at which the origin of the membrane height has been chosen. After solving this system, the total membrane free energy has to be minimized with respect to the free parameters h_0 and β . Assuming revolution symmetry, the general distortion energy (32) within the Wigner-Seitz cell takes the form

$$\begin{aligned} \mathcal{H}_{hm} = \pi \bigg[& \kappa(r \ddot{h} + \dot{h})\dot{h} - \kappa h(r \ddot{\theta} + \dot{\theta} - \dot{h}/r) \\ & - \gamma(r \dot{\theta} + \theta)\dot{h} + \gamma h(r \ddot{\theta} + \dot{\theta} - \dot{h}/r) \\ & - \gamma(r \ddot{h} + \dot{h})\theta + K_1 r \theta \dot{\theta} + K_1 \theta^2 \bigg]_{r_0}^R, \end{aligned} \quad (78)$$

where all the terms taken in $r = R$ vanish due to the boundary conditions. The interaction has the following scaling property:

$$\frac{\mathcal{H}_{hm}}{\pi \kappa \Theta^2} = \overline{\mathcal{H}}_{hm} \left(\mu, \frac{r_0}{\xi_\theta}, \frac{R}{\xi_\theta} \right). \quad (79)$$

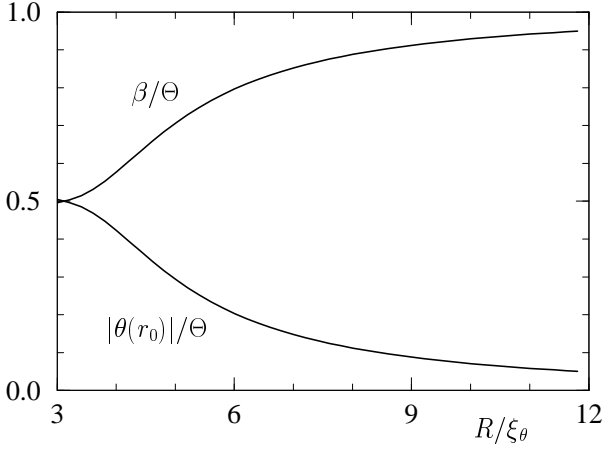


Fig. 17. Boundary tilt $\theta(r_0)$ and boundary membrane inclination β as a function of the distance R between the inclusion. The inclusions radius is $r_0 = 3\xi_\theta (\simeq 60 \text{ \AA})$ and the tilt-shape coupling γ is zero.

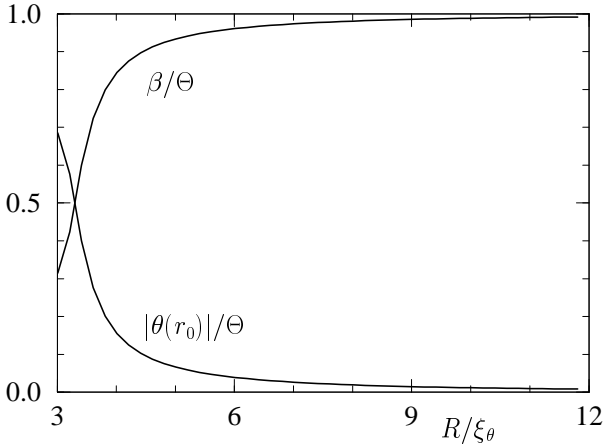


Fig. 18. Same as Fig. 17, however in the presence of a strong shape-tilt coupling corresponding to $\mu = 0.9$.

The results are the following. Even in the absence of a shape-tilt coupling, there is a trade between the shape and the tilt modes, which is due to the boundary condition (74). The membrane tends to develop a tilt close to the inclusions in order to flatten its shape. The typical solution for the membrane shape resembles that sketched in Fig. 16. The boundary tilt relaxes on a distance $\simeq 4q^{-1}$, typically of order a few ξ_θ 's unless μ is close to 1. The boundary tilt is a function of the separation R between the inclusions. When $R \gg \xi_\theta$, the amplitude of the boundary tilt $\theta(r_0)$ is negligible: the membrane curvature, which is small, only exerts a weak torque on the tilt. Conversely, when the inclusions are close to contact, the boundary tilt is a finite fraction of the inclusions average cone angle Θ . For $K_1 = \kappa$, as we have assumed, this fraction is exactly $1/2$ for $\mu = 0$ (Fig. 17).

In the presence of a strong shape-tilt coupling (μ close to 1), the tilt relaxes on a distance q^{-1} significantly shorter than ξ_θ , and the boundary tilt $\theta(r_0)$, which gets somewhat larger at contact, actually relaxes more rapidly with the

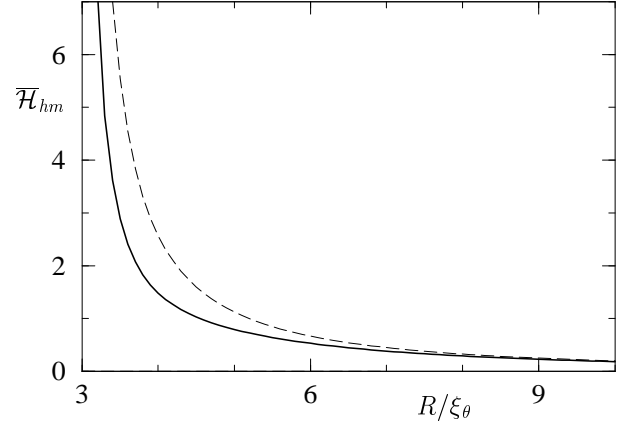


Fig. 19. Normalized interaction energy per inclusion $\overline{\mathcal{H}}_{hm}$ vs. inclusions separation R . The inclusions radius is $r_0 = 3\xi_\theta (\simeq 60 \text{ \AA})$ and the tilt-shape coupling $\gamma = 0$. The dashed curve corresponds to the case where the tilt is not allowed.

distance between the inclusions (Fig. 18). Thus, except when the inclusions are very close to one another, the tilt is rapidly negligible. The reason is that the tilt set in order to flatten the membrane is *always* costly from the point of view of the $-\gamma \nabla^2 h (\nabla \cdot \mathbf{m})$ coupling (when $\gamma > 0$). Hence the coupling does not favor an expansion of the tilt distortion, while in the preceding section the dilation-tilt-difference coupling did favor an expansion of the tilt-difference for $x < 0$, which produced spectacular effects.

Let us estimate the magnitude of the interaction energy, which is given by the normalization factor $\pi\kappa\Theta^2$ in (79). With $\xi_\theta \simeq 20 \text{ \AA}$, a typical protein size $r_0 = 3\xi_\theta (\simeq 60 \text{ \AA})$ and $\Theta \simeq 10^\circ$, we obtain $\pi\kappa\Theta^2 \simeq 2.5 k_B T$. Figure 19 shows the interaction energy per inclusion in the case of zero shape-tilt coupling. The interaction is always repulsive; it diverges at small separations as $(R - r_0)^{-1}$ and tends asymptotically towards the exact form

$$\mathcal{H}_h = 2\pi\kappa\Theta^2 \frac{r_0^2}{R^2 - r_0^2}, \quad (80)$$

which can be calculated analytically by completely neglecting the tilt. As it is apparent in Fig. 19, the tilt relaxes some of the interaction energy at short inclusions separations. For $\mu \rightarrow 1$, we find that $\mathcal{H}_{hm} \rightarrow \mathcal{H}_h$ at all separations. The effect of the tilt is therefore negligible.

4 Conclusions

We have developed an elastic model for membranes that describes at the same level large- and short-scale distortions of the bilayer. Strictly speaking, such a continuum theory at a molecular scale should not be expected to give more than semi-quantitative results (see Sec. 2.6). Nevertheless our hope is that the theory captures the qualitative trends of the competitions between the different elastic variables. Using a systematic expansion in the monolayers profiles and tilts, we have shown that the average

membrane shape (h) is coupled to the average molecular tilt (\mathbf{m}), both being decoupled (at lowest order) from the membrane dilation (u) and the difference in the monolayers tilts ($\hat{\mathbf{m}}$), which are coupled together.

We have used this model to study the contribution of the membrane elasticity to the short- and long-range interactions among inclusions. Because the boundary conditions at a membrane inclusion are decoupled in the same way as the elastic variables, the interaction energy can be calculated as simply the sum of a dilation-tilt-difference contribution ($u-\hat{\mathbf{m}}$) and a shape-tilt contribution ($h-\mathbf{m}$).

Membrane inclusions generally have a slightly convex or concave hydrophobic core of thickness different from that of the bilayer. Such inclusions will excite the coupled dilation-tilt-difference ($u-\hat{\mathbf{m}}$) mode. The thickness mismatch creates an energetic dilation corona around the inclusions and yields an *attraction* between like inclusions: no extra distortion occurs when the coronas overlap since the boundary dilations match. The tilt-difference, however, yields a *repulsion* between like inclusions: going from α_0 to $-\alpha_0$, it develops a strong gradient when the coronas overlap. Inclusion producing no tilt-difference aggregate, while inclusions producing a nonzero tilt-difference either repel one another or favor $2D$ crystals. The latter situation arises for small tilt-differences, or when the dilation corona extends further than the tilt-difference corona.

When the dilation-tilt-difference coupling is large, the distortions in the coronas exhibit damped oscillations. This effect occurs because of the vicinity of a “ripple” instability in which both the membrane dilation and tilt-difference become unstable. The inter-particle potential develops then several minima, which implies the possible coexistence of different crystals of inclusions having different lattice spacings. The latter can be significantly larger than the inclusions size. The inclusions most likely to form $2D$ crystals are those with either a *long-convex* or a *short-concave* hydrophobic core, i.e., those disfavored from the point of view of the $c\nabla u \cdot \hat{\mathbf{m}}$ coupling. This is because the gradient of u being more costly, the dilation corona extends (favoring “long-range” attraction), while at the same time the dilation corona shrinks (making the repulsion occur only at smaller separations). Conversely, short-convex and long-concave inclusions have a dominant repulsion and should form disordered phases.

Membrane inclusions generally have also a slightly conical shape. Hence they excite the coupled shape-tilt ($h-\mathbf{m}$) mode. In first approximation, the conical shape constrains the membrane to depart with a contact angle Θ relative to the inclusion axis. The energy stored in the curvature of the membrane yields a repulsion between like inclusions in an array that diverges at short distances as R^{-1} and fall off as R^{-2} . This is a many body effect, since the interaction between a pair of inclusions falls off more rapidly, as R^{-4} [19]. In the latter case, the inclusions axes rotate away from one another in order to minimize the curvature energy of the membrane. In an array of inclusions this rotation is zero by symmetry.

If we allow for a tilt of the lipids, the membrane can depart with a smaller contact angle β . In order to remain

parallel to the inclusions boundaries, the lipids tilt then by $\beta - \Theta$. When the inclusions are far apart, the tilt is completely negligible since the torque exerted by the membrane curvature on the tilt is weak. Conversely, when the inclusions are distant a few times the membrane thickness, the tilt becomes a finite fraction of Θ . The interaction energy is then reduced, however there is no qualitative change in the interaction potential. As for the shape-tilt coupling $-\gamma \nabla^2 h (\nabla \cdot \mathbf{m})$, it reduces the relaxation length of the tilt and simply reduces its effects. The reason is that the tilt set in order to flatten the membrane is always costly from the point of view of the coupling, for the expected positive sign of γ . Hence the tilt does not propagate far away of the inclusions in the vicinity of the ripple instability (where both the shape and tilt modes become unstable).

Acknowledgments

Useful discussions with A. Ajdari, P. Pincus and L. Peliti are gratefully acknowledged. This work was partially supported by the NSF Grants No. MRL DMR 91-23048 and 96-24091, and by the CNRS.

References

1. J. N. Israelachvili, *Intermolecular and Surface Forces* (Academic Press, London, 1992).
2. S. A. Safran, *Statistical Thermodynamics of Surfaces, Interfaces and Membranes* (Addison-Wesley, Reading, MA, 1994).
3. L. Peliti, in *Fluctuating Geometries in Statistical Mechanics and Field Theory*, edited by F. David, P. Ginsparg, and J. Zinn-Justin (Les Houches session LXII, Elsevier Science, 1996).
4. P. Canham, *J. Theo. Bio.* **26**, 61 (1970).
5. W. Helfrich, *Z. Naturforsch.* **28C**, 693 (1973).
6. *Statistical Mechanics of Membranes and Surfaces*, D. Nelson, T. Piran, and S. Weinberg, eds. (World Scientific, Singapore, 1989).
7. S. Marčelja, *Biophys. Acta* **455**, 1 (1976).
8. J. C. Owicki and H. M. McConnell, *Proc. Natl. Acad. Sci. USA* **76**, 4750 (1979).
9. H. W. Huang, *Biophys. J.* **50**, 1061 (1986).
10. N. Dan, P. Pincus, and S. A. Safran, *Langmuir* **9**, 2768 (1993).
11. N. Dan, A. Berman, P. Pincus and S. A. Safran, *J. Phys. II France* **4**, 1713 (1994).
12. H. Aranda-Espinoza, A. Berman, N. Dan, P. Pincus and S. A. Safran, *Biophys. J.* **71**, 648 (1996).
13. These variables have been introduced in another context by U. Seifert, J. Shillcock, and P. Nelson, *Phys. Rev. Lett.* **77**, 5237 (1996).
14. J.-B. Fournier, *Europhys. Lett.* **43** (6), 725 (1998).
15. F. David and S. Leibler, *J. Phys. II France* **1**, 959 (1991).
16. Note that in [11] the $(\nabla u)^2$ term would be restored if the lowest order term of the u -expansion would be considered a function $f_0(\Sigma, (\nabla \Sigma)^2)$ of the area per molecule and its gradient.
17. T. C. Lubensky and F. C. MacKintosh, *Phys. Rev. Lett.* **71**, 1565 (1993).

18. C.-M. Chen, T. C. Lubensky and F. C. MacKintosh, Phys. Rev. E **51**, 504 (1995).
19. M. Goulian, R. Bruinsma, and P. Pincus, Europhys. Lett. **22**, 145 (1993); Erratum: **23**, 155 (1993); Comment: J. B. Fournier and P. G. Dommersnes, Europhys. Lett. **39**, 681 (1997).
20. J. M. Park and T. C. Lubensky, J. Phys. I France **6**, 1217 (1996).
21. R. R. Netz, J. Phys. I France **7**, 833 (1997).
22. In principle one should consider the free energy per surface unit \mathcal{H}/R^2 , however this does not change significantly the position of the energy minimum.